Progress In Electromagnetics Research M, Vol. 103, 81–90, 2021

Bandpass Unconditionally Stable CE-BOR-PML Scheme with CNDG Algorithm for Rotational Symmetric Simulation

Shihong Wu[1, *], Lining Liu[1], Yunyun Dong[1], Feng Su[1], and Xiangguang Chen[1, 2]

Abstract—Unconditionally stable approximate Crank-Nicolson (CN) perfectly matched layer (PML) implementation is proposed to treat open region problems for a bandpass rotational symmetric structure. To be more specific, this implementation is based upon the CN Douglas-Gunn (DG) procedure and the complex envelope (CE) method in body of revolution (BOR) finite-difference time-domain (FDTD) lattice. The proposed scheme inherits the advantages of the CNDG procedure, CE method, and BOR-FDTD algorithm which can improve the efficiency, enhance the absorption, and maintain the calculation accuracy. The effectiveness which includes accuracy, efficiency, occupied resources, and absorption is illustrated through a numerical example. The numerical results reveal that the proposed scheme provides considerable accuracy, creditable absorption, and outstanding efficiency. Meanwhile, it can also verify that the proposed scheme is stable without the limitation of Courant-Friedrich-Levy (CFL) condition.

1. INTRODUCTION

The finite-difference time-domain (FDTD) algorithm shows its great potential in wide-band simulation of the rectangular coordinate system. According to the Yee's grid, hexahedral mesh generation leads to the decrement of accuracy and efficiency in circular symmetry structures [1]. To alleviate such condition, body of revolution FDTD is regarded as the most powerful method in the simulation of circular symmetry structures. According to the BOR-FDTD algorithm, three-dimensional problems can be projected into two-dimensions resulting in the significant improvement especially in efficiency [2].

By applying the BOR-FDTD algorithm to bandpass problems, time step must be obtained according to the maximum frequency resulting in unacceptable simulation duration and accuracy [3]. Complex envelope (CE) method is introduced to overcome these drawbacks [4]. According to the CE method, the time step can be maximized according to the bandwidth of source rather than the maximum frequency. As a time explicit algorithm, the stability of the BOR-FDTD algorithm is limited by the Courant-Friedrichs-Levy (CFL) condition [5]. Without the satisfaction of CFL condition, BOR-FDTD algorithm will become non-convergence resulting in invalid calculation. By employing such an algorithm to fine structures and multi-scale problems, a large number of time steps must be calculated resulting in expensive computation. Unconditionally stable algorithms are proposed to remove the CFL limit. Until now, several prevalent unconditionally stable algorithms have been proposed to efficiently solve the Maxwell's equations including the alternating-direction implicit (ADI), locally one-dimensional (LOD), split-step (SS) algorithms, etc. [6–8]. As can be concluded, the original ADI, LOD, SS schemes are implemented by the split step procedure. Such condition results in the degeneration of accuracy and efficiency. As a one-step procedure, original Crank-Nicolson (CN) scheme which can solve the Maxwell's equations within a single step has become prevalent than ever before [9]. Compared with the other original schemes, the original CN scheme shows better efficiency and accuracy. The original CN is

Received 14 May 2021, Accepted 2 June 2021, Scheduled 5 July 2021
* Corresponding author: Shihong Wu (shihongwu@hotmail.co.jp).
[1] Department of Electrical and Electronic Engineering, College of Engineering, Yantai Nanshan University, Longkou 265713, China.
[2] School of Chemistry and Chemical Engineering, Beijing Institute of Technology, Beijing 100081, China.

merely efficient in one-dimension, due to the forming of large sparse matrices in multi-dimensions [10]. In order to avoid the calculation and generation of large sparse matrices, approximate CN scheme is carried out which shows considerable entire performance in terms of accuracy and efficiency compared with the original ADI, LOD, and SS schemes. The approximate CN schemes are firstly proposed in two dimensions including approximate-decoupling (AD) and Douglas-Gunn (DG) schemes [11, 12]. However, approximate CN schemes cannot be directly extended into three dimensions [13]. Several approximate CN schemes have been developed in three dimensions including cycle-sweep-uniform (CSU), approximate-factorization-splitting (AFS), and direct splitting (DS) [14, 15]. However, it has been testified that the CNCSU scheme is conditionally stable [16–18]. Series of investigations have been developed which are mainly based on the approximate CN schemes [19–25]. As can be concluded, they are mainly for the rectangular coordinate system. For the rotational symmetric simulation, several implementations have been carried out including the original ADI and CNAD schemes [26, 27]. Compared with the ADI scheme, approximate CN scheme shows less numerical dispersion error with larger time steps [11, 12]. The CNDG method is implemented by adding disturbance terms at both sides of the equations. Such operation results in the decrement of efficiency and increment of accuracy. Thus, compared with the CNAD scheme, CNDG can be regarded as the compromise between the efficiency and accuracy [28].

For the simulation of open regions in finite space, the absorbing boundary condition must be employed to terminate the unbounded lattice [5]. Among several absorbing boundary conditions, perfectly matched layer (PML) can be regarded as the most popular one [29–31]. The original PML is a split-field implementation which shows limitation in absorption and efficiency [32]. During the simulation, six auxiliary variables must be introduced which also indicates the degeneration of entire performance. To alleviate such condition, the unsplit-field formulation including stretched coordinate and complex-frequency-shifted (CFS) PMLs are proposed in recent past decades [33, 34]. It has been testified that the unsplit-field scheme shows its advantages in simplifying the implementation at corners and edges, absorbing low-frequency evanescent waves and reducing late-time reflections. To our knowledge, the bandpass form for the BOR-FDTD algorithm has not been investigated [35–37].

Here, by incorporating CE method, CNDG scheme and BOR-FDTD algorithm, unconditionally stable implementation is proposed for the open region problems in bandpass rotational symmetric simulation. The scheme is proposed to take full advantage of them in terms of considerable accuracy, creditable absorption, and outstanding efficiency. The effectiveness and efficiency are demonstrated through the numerical example.

2. FORMULATION

In the PML region for TM_ϕ wave, the frequency-domain Maxwell's equations can be given as

$$-j\omega\mu_0 H_r = -\frac{1}{S_z}\frac{\partial E_\varphi}{\partial z} \tag{1a}$$

$$-j\omega\mu_0 H_z = \frac{1}{S_r}\frac{\partial E_\varphi}{\partial r} + \frac{E_\varphi}{\tilde{r}} \tag{1b}$$

$$j\omega\varepsilon_0 E_\varphi = \frac{1}{S_z}\frac{\partial H_r}{\partial z} - \frac{1}{S_r}\frac{\partial H_z}{\partial r} \tag{1c}$$

where ε_0 and μ_0 are the relative permittivity and permeability, respectively. $S_\eta, \eta = r, \varphi, z$ is the stretched coordinate variable with CFS factor which can be defined as

$$S_\eta = \kappa_\eta + \frac{\sigma_\eta}{\alpha_\eta + j\omega\varepsilon_0} \tag{2}$$

where σ_η and α_η are assumed to be positive real, and $\kappa_\eta \geq 1$ is real. Within Eq. (1b), $\tilde{r}$ is the complex spatial coordinate-stretching variable, given as

$$\tilde{r} = r_1 + \int_{r_1}^{r} S_r(r')dr' \tag{3}$$

where r_1 represents the distance between the FDTD lattice and the PML regions in r-direction. According to the partial fraction method, the multiplicative inverse of S_η can be given as

$$S_\eta^{-1} = k_\eta \frac{j\omega + a_\eta}{j\omega + b_\eta} \tag{4}$$

where $k_\eta = 1/\kappa_\eta$, $a_\eta = \alpha_\eta/\varepsilon_0$, and $b_\eta = a_\eta + a_\eta/\kappa_\eta$. By substituting Eq. (4) into Eqs. (1a)–(1c), one obtains

$$j\omega\mu_0 H_r = k_z \frac{j\omega + a_z}{j\omega + b_z}\frac{\partial E_\varphi}{\partial z} \tag{5a}$$

$$-j\omega\mu_0 H_z = k_r \frac{j\omega + a_r}{j\omega + b_r}\frac{\partial E_\varphi}{\partial r} + \frac{E_\varphi}{\tilde{r}} \tag{5b}$$

$$j\omega\varepsilon_0 E_\varphi = k_z \frac{j\omega + a_z}{j\omega + b_z}\frac{\partial H_r}{\partial z} - k_r \frac{j\omega + a_r}{j\omega + b_r}\frac{\partial H_z}{\partial r} \tag{5c}$$

To update the equations inside PML regions, the introduction of auxiliary variables is employed, given as

$$j\omega\mu_0 H_r = (j\omega + a_z)\, G_z \tag{6a}$$

$$-j\omega\mu_0 H_z = (j\omega + a_r)\, G_r + \frac{E_\varphi}{(\lambda_r \tilde{r})} - G_{\tilde{r}} \tag{6b}$$

$$j\omega\varepsilon_0 E_\varphi = (j\omega + a_z)\, F_z - (j\omega + a_r)\, F_r \tag{6c}$$

where auxiliary variables are given as, for example,

$$j\omega F_z + b_z F_z = k_z \frac{\partial H_r}{\partial z} \tag{7a}$$

$$j\omega G_z + b_z G_z = k_z \frac{\partial E_\varphi}{\partial z} \tag{7b}$$

$$j\omega G_{\tilde{r}} + \frac{\alpha_r}{\varepsilon_0} G_{\tilde{r}} + \frac{\theta_r}{(\varepsilon_0 \lambda_r)} G_{\tilde{r}} = \frac{\theta_r}{(r\varepsilon_0 \lambda_r^2)} E_\varphi \tag{7c}$$

where $\lambda_r = \frac{1}{r} \cdot (r_1 + \int_{r_1}^{r} \kappa_r(r')dr')$ and $\theta_r = \frac{1}{r} \cdot \int_{r_1}^{r} \sigma_r(r')dr'$. By introducing the CE method, the bandpass signal can be expressed by the relationship $\Phi = \mathrm{Re}\{\hat{\Phi} e^{j\varpi t}\}$, where $\mathrm{Re}\{\cdot\}$ is the real part of the equation, ϖ the carrier frequency, Φ the broadband signal, and $\hat{\Phi}$ the bandpass complex envelope signal. By transforming Eqs. (6a)–(6c) and (7a)–(7c) into time domain according to the relationship $j\omega \leftrightarrow \partial_t$, employing the CE method and CN scheme in the resultants, and substituting Eqs. (7a)–(7c) into Eqs. (6a)–(6c), the results can be obtained as

$$\hat{H}_r^{n+1} = c_1 \hat{H}_r^n + p_{1hz} \hat{G}_z^n + p_{2hz} \delta_z \left(\hat{E}_\varphi^{n+1} + \hat{E}_\varphi^n\right) \tag{8a}$$

$$\hat{H}_z^{n+1} = c_1 \hat{H}_z^n + p_{1hr} \hat{G}_r^n + p_{2hr} \delta_r \hat{E}_\varphi^{n+1} - p_{2hr} \partial_r \hat{E}_\varphi^n + p_{3hr} \partial_r \hat{E}_\varphi^n + p_{4hr} \hat{G}_{\tilde{r}}^n \tag{8b}$$

$$\hat{E}_\varphi^{n+1} = c_1 \hat{E}_\varphi^n + p_{1ez} \hat{F}_z^n + p_{2ez} \delta_z \left(\hat{H}_r^{n+1} + \hat{H}_r^n\right) - p_{1er} \hat{F}_r^n - p_{2er} \delta_r \left(\hat{H}_z^{n+1} + \hat{H}_z^n\right) \tag{8c}$$

where $c_1 = (2 - j\varpi\Delta t)/(2 + j\varpi\Delta t)$, $c_2 = 2 + j\varpi\Delta t$, $p_{1h\eta} = 2\Delta t(a_\eta - b_\eta)/(c_2\mu_0)$, $p_{2h\eta} = 2\Delta t k_\eta/(c_2\mu_0)$, $p_{3h\eta} = \Delta t/(ic_2\lambda_\eta)$, $p_{4hr} = 2\Delta t/c_2$, $p_{1e\eta} = 2\Delta t(a_\eta - b_\eta)/(c_2\varepsilon_0)$, $p_{2e\eta} = 2\Delta t k_\eta/(c_2\varepsilon_0)$. The auxiliary variables can be given as

$$\hat{F}_z^{n+1} = p_{5z} \hat{F}_z^n + p_{6z} \delta_z \hat{H}_r \tag{9a}$$

$$\hat{G}_z^{n+1} = p_{5z} \hat{G}_z^n + p_{6z} \delta_z \hat{E}_\varphi \tag{9b}$$

$$\hat{G}_{\tilde{r}}^{n+1} = p_{7\tilde{r}} \hat{G}_{\tilde{r}}^n + p_{8\tilde{r}} \frac{\delta \hat{E}_\varphi^n}{(2i)} \tag{9c}$$

where $p_{5\eta} = (2 - j\varpi\Delta t - b_\eta\Delta t)/(2 + j\varpi\Delta t + b_\eta\Delta t)$, $p_{6\eta} = 2\Delta t k_\eta/(2 + j\varpi\Delta t + b_\eta\Delta t)$, $p_{7\tilde{r}} = (2\varepsilon_0\lambda_r - j\varpi\Delta t - \alpha_r\Delta t\lambda_r - \theta_\eta\Delta t)/(2\varepsilon_0\lambda_r + j\varpi\Delta t + \alpha_r\Delta t\lambda_r + \theta_r\Delta t)$ and $p_{8\tilde{r}} = 2\theta_r\Delta t/[\Delta r\lambda_r(2\varepsilon_0\lambda_r + j\varpi\Delta t + \alpha_r\Delta t\lambda_r + \theta_r\Delta t)]$. The operator δ_η is the first-order finite-difference form, for example,

$$\delta_r \hat{E}_\varphi^n = \left(\hat{E}_{\varphi(i+1,k)}^n - \hat{E}_{\varphi(i,k)}^n\right) \Big/ (2\Delta r) \tag{10}$$

It can be observed that Eqs. (8a)–(9c) can be updated directly. However, large sparse matrices are formed at each time step resulting in much expensive calculation. Such a phenomenon becomes unpractical. In order to avoid the calculation of such matrices and improve the entire efficiency, the approximate CN scheme is employed which is the CNDG scheme. By substituting Eqs. (8a) and (8b) into Eq. (8c), one obtains

$$\begin{aligned}(1-D_{2r}-D_{2z})\,\hat{E}_{\varphi}^{n+1} &= (c_1+D_{2z}+D_{2r})\,\hat{E}_{\varphi}^{n}+p_{1ez}\hat{F}_z^n-p_{1er}\hat{F}_r^n-p_{1hr}p_{2er}\delta_r\hat{G}_r^n+p_{1hz}p_{2ez}\delta_z\hat{G}_z^n\\ &\quad -p_{4hr}p_{2er}\delta_r\hat{G}_{\tilde{r}}^n-p_{3hr}\delta_r\delta_r\hat{E}_{\varphi}^n+(1+c_1)\,p_{2ez}\delta_z\hat{H}_r^n-(1+c_1)\,p_{2er}\delta_r\hat{H}_z^n \quad (11)\end{aligned}$$

where $D_{2\eta}=p_{2e\eta}p_{2h\eta}\delta_{2\eta}$. By adding the disturbance terms $D_{2r}D_{2z}\hat{E}_{\varphi}^{n+1}$ and $D_{2r}D_{2z}\hat{E}_{\varphi}^{n}$ at both sides of the equations, the resultants can be updated by employing sub-steps as

$$(1-D_{2r})\,w = (c_1+D_{2r}+2D_{2z})\,\hat{E}_{\varphi}^{n}+\mathbf{A}^n \quad (12a)$$

$$(1-D_{2z})\,\hat{E}_{\varphi}^{n+1} = w-D_{2z}\hat{E}_{\varphi}^{n} \quad (12b)$$

where w is the temporary variable, and $\mathbf{A}^n$ is the other components at right sides of equations with the n-th time step. It can be observed that tri-diagonal matrices are formed at left side of Eqs. (12a) and (12b) which can be solved directly by employing the Thomas algorithm implicitly resulting in the improvement of entire computational efficiency [38].

3. NUMERICAL RESULTS

For the demonstration of effectiveness which includes the absorption and efficiency of different PML algorithms, a numerical example is studied. Here, the coaxial transmission line is introduced whose sketch picture is shown in Fig. 1. As shown in Fig. 1(a), the entire structure is rotationally-symmetric along z-axis which can be converted to 2-D according to the BOR-FDTD algorithm. Fig. 1(b) shows the computational domain and its detail parameters.

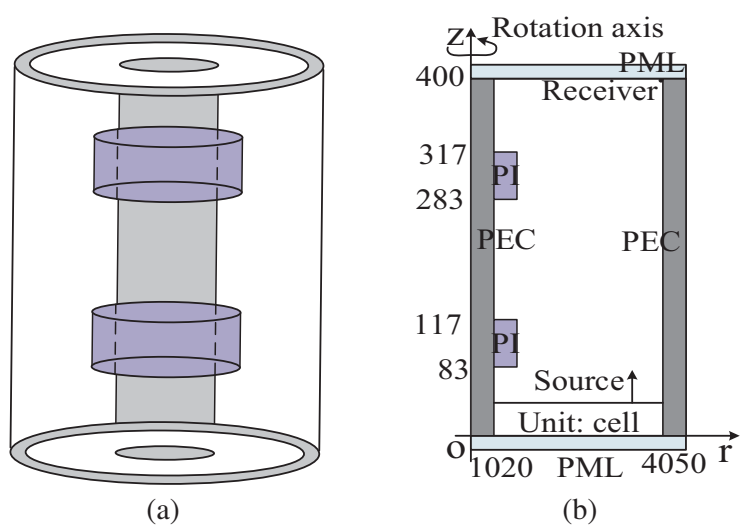

Figure 1. The sketch picture of coaxial transmission line. (a) Entire structure. (b) FDTD computational domain.

The coaxial transmission line is composed of cylinders with materials including polyimide (PI) with the electric parameters of $\varepsilon_r = 3.4$ and perfect electric conductor (PEC). The middle of the structure is PEC cylinder with the radius and height of 0.3 mm and 12 mm, respectively. Two PI cylinder structures with inner radius, outer radius, and height of 0.3 mm, 0.6 mm, and 1 mm are located at 2.5 mm to 3.5 mm, 8.5 mm to 9.5 mm along z-axis, respectively. At the boundary of coaxial transmission line, a PEC cylinder with the height and thickness of 12 mm and 0.3 mm is employed. It can be observed that

the structure can be regarded as a rotational symmetric structure. Thus, the structure can be converted into two dimensions according to the BOR-FDTD algorithm, as shown in Fig. 1(b).

The two-dimensional structure has dimensions of $50\Delta r \times 400\Delta z$ in r- and z-directions, respectively. The PEC bulks with the size of $10\Delta r \times 400\Delta z$ are located at the left and right boundaries. The PI bulks which have dimensions of $10\Delta r \times 34\Delta z$ are located at 83 to 117, 283 to 317 of z-direction. The incident wave which is a modulated Gaussian pulse with the center frequency f_0 and maximum frequency of 15 GHz and 20 GHz propagates along positive z-direction. Thus, the percent bandwidth $\%B$ can be calculated as 66.7. The receiver point is located at the left top corner with the distance of one cell from the side of PML regions to observe the wave propagation and evaluate wave reflections. Because the PML regions can simulate the infinite extension of the computational domain, the wave reflection generated by PML regions can be employed to the evaluation of entire performance. For comparison, several different PML algorithms are carried out in this section. They include the conventional CFS-PML in BOR-FDTD algorithm (FDTD-PML) in [39], the CFS-PML in original ADI algorithm (ADI-PML) in [26], the CFS-PML in CNAD algorithm in [27], the uniaxial PML (UPML-HFSS) of HFSS in [40], the convolutional PML (CST-CPML) of CST in [41], and the Mur absorbing boundary condition (Mur) in [29]. For clarify illustration, the proposed scheme is denoted as CE-CNDG-PML. Inside the PML regions, the parameters are selected to obtain the best performance both in time domain and frequency domain. The parameters of them are selected as $\kappa_\eta = 21$, $\alpha_\eta = 1.1$, $m_\eta = 2$, $\sigma_{\eta_\max} = 0.4\sigma_{\eta_opt}$, where

$$\sigma_{\eta_opt} = (m_\eta + 1)/(150\pi\Delta\eta) \tag{13}$$

In the unconditionally stable algorithms, the mesh size can be selected by the accuracy of calculation rather than the CFL condition. Thus, the mesh size is chosen as $\Delta r = \Delta z = \Delta = 3 \times 10^{-5}$ m. The time step of the conventional FDTD algorithm is $\Delta t_{\max}^{FDTD} = 0.95\Delta/(2c_0) = 47.5$ fs. The time step of CE method $\Delta t_{\max}^{CE}$ can be obtained as 190 fs which can be observed as $\Delta t_{\max}^{CE} = 4\Delta t_{\max}^{FDTD}$. The CFL number is defined as $CFLN = \Delta t/\Delta t_{\max}^{FDTD}$, where Δt is the time step of the unconditionally stable FDTD algorithm. Figs. 2(a) and (b) show the waveform at the receiver obtained by different PML algorithms and CFLNs.

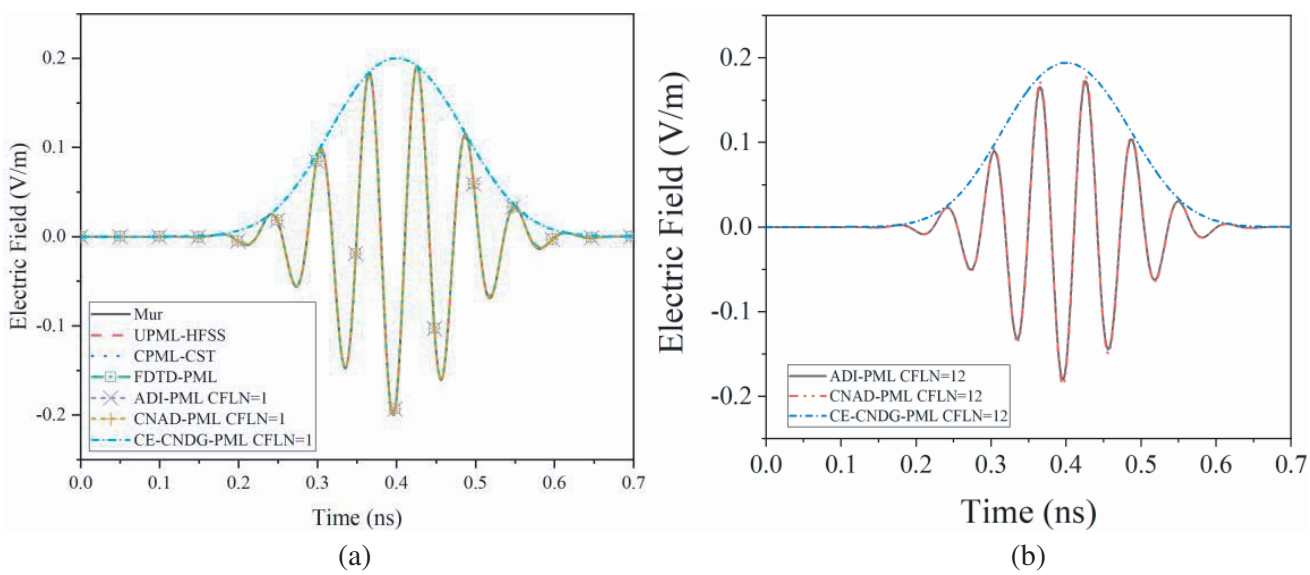

Figure 2. The waveform obtained by Mur, UPML-HFSS, CST-CPML, FDTD-PML, ADI-PML, CNAD-PML, CE-CNDG-PML CFLN = 1 and 12, respectively.

Through the result, it can be observed that the envelope can be obtained according to the CE method. Meanwhile, it can be observed that the waveforms obtained by different algorithms are overlapped. The waveform obtained by the proposed scheme is overlapped with the upper boundary of the waveform obtained by the other algorithms. In addition, the waveform with larger CFLNs shows

less shifting than Mur, UPML-HFSS, CST-CPML, and FDTD-PML. Such a phenomenon indicates that the proposed scheme can obtain considerable accuracy during the entire time domain simulation. As demonstrated previously, the performance of different PML algorithms can be demonstrated by the wave reflection or the wave absorption. The absorption and wave reflections inside PML regions can be evaluated by the relative reflection error which can be defined as

$$R_{dB}(t) = 20\log_{10}\left[\left|E_z^t(t) - E_z^r(t)\right| / \left|\max\left\{E_z^r(t)\right\}\right|\right] \tag{14}$$

where $E_z^t(t)$ is the test solution which can be directly obtained by different PML algorithms, and $E_z^r(t)$ is the reference solution. The reference solution can be directly obtained by enlarging the computational domain by 20 times and employing thicker PML regions for the termination with 128 cells without changing the relative position between the source and receiver. During the calculation of reference solution, the reflection wave at the receiver can be ignored due to the enlarged domain and thicker PML regions. Fig. 3 shows the relative reflection error in the time domain obtained by different PML algorithms and CFLNs.

For clearness, the simulation time of 0.5 ns is shown in Fig. 3. The absorption can be evaluated by both of the maximum reflection error (MRRE) and late-time reflections. Fig. 3(a) shows the absorption in the time domain obtained by Mur, UPML-HFSS, CST-CPML, and FDTD-PML. It can be observed that the Mur absorbing boundary condition shows the worst absorption during the entire time simulation. Compared with the HFSS-UPML, CPML-CST can obtain considerable absorption

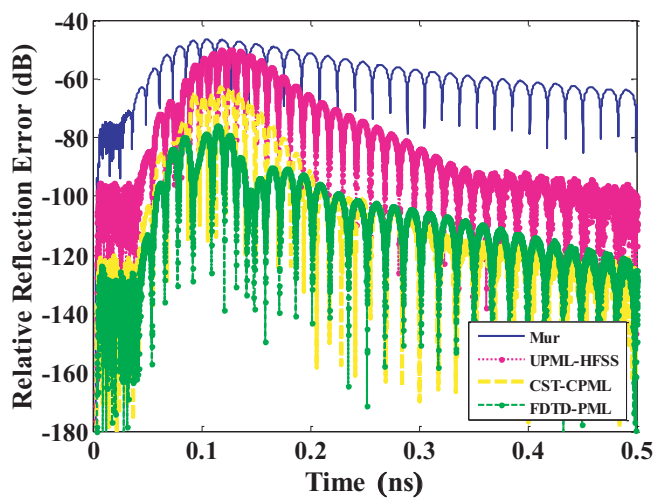

(a)

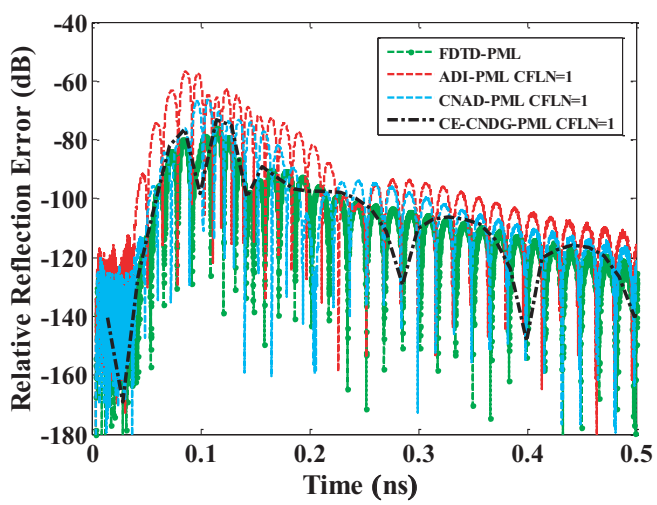

(b)

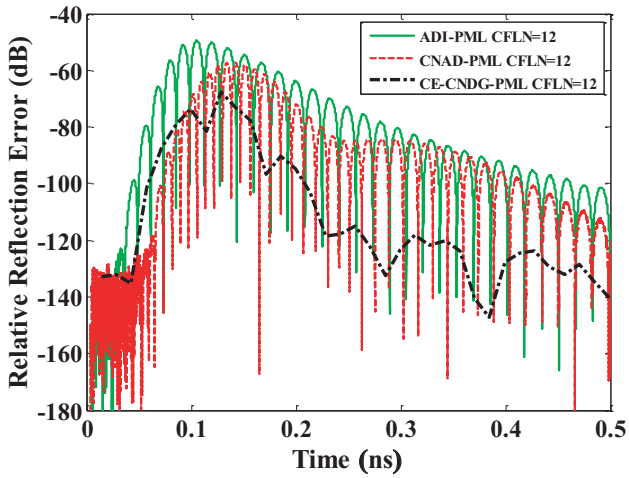

(c)

Figure 3. The relative reflection error in the time domain obtained by (a) Mur, UPML-HFSS, CPML-CST and FDTD-PML, (b) FDTD-PML, ADI-PML, CNAD-PML, CE-CNDG-PML CFLN = 1, (c) FDTD-PML, ADI-PML, CNAD-PML, CE-CNDG-PML CFLN = 12.

indicating that the CPML shows better performance than the UPML. The FDTD-PML has the best performance among these implementations. Fig. 3(b) shows the absorption of FDTD-PML, ADI-PML, CNAD-PML, and proposed scheme with CFLN = 1. It can be observed that the ADI-PML and CNAD-PML have inferior absorption to the others, while FDTD-PML and the proposed scheme are the same. Such condition indicates that the proposed scheme is efficient compared with the ADI-PML and CNAD-PML. As can be observed from Fig. 3(c), the absorption decreases significantly especially with larger CFLNs. The reason is that the numerical dispersion increases with larger time steps resulting in such condition. The computational efficiency and resource are shown in Table 1. It can be observed that the iteration steps of the unconditionally stable algorithms can be decreased with larger time steps resulting in the improvement of entire efficiency. It should be noticed that the efficiency of proposed scheme is better than FDTD-PML. Furthermore, it should be noticed that the ADI scheme for comparison is based on the original scheme which means that it has very complex operation manipulations. Until now, many implementations have been proposed to improve the efficiency of the ADI algorithm including the leapfrog ADI, the fundamental ADI, etc. [42–44]. Within these algorithms, the complex manipulations

Table 1. Comparison of CPU time, iteration steps, memory, reduction and MRRE of different PML algorithms.

	CFLN	Iteration Steps	Time (s)	Memory (MB)	Reduction (%)
FDTD-PML	1	65536	79.4	11.7	-
Mur	1	65536	51.3	9.9	35.4
UPML-HFSS	1	65536	85.1	11.8	−7.2
CPML-CST	1	65536	82.6	11.8	−4.0
ADI-PML	1	65536	201.6	13.9	−153.9
CNAD-PML	1	65536	189.0	13.5	−138.0
Proposed	1	16384	52.7	14.2	33.6
ADI-PML	12	5462	19.2	13.9	75.8
CNAD-PML	12	5462	17.1	13.5	78.5
Proposed	12	1366	10.8	14.2	86.4

can be simplified to make the ADI scheme more efficient. Most specifically, while the ADI-PML method has not been simplified as compared to the CNDG here, more efficient schemes can be implemented following References [45–50].

4. CONCLUSION

Here, by incorporating the CE method, CNDG procedure, and BOR-FDTD algorithm, an unconditionally stable PML scheme is proposed for the termination of unbounded domain in bandpass simulation. The proposed scheme is to take advantage of them in terms of considerable accuracy, creditable absorption, and outstanding efficiency. Through the numerical example, it can be demonstrated that the proposed scheme can obtain outstanding performance. Meanwhile, the proposed scheme can maintain its stability with the enlargement of CFLNs which indicates that it is an unconditionally stable implementation.

ACKNOWLEDGMENT

This work was supported in part by National Natural Science Foundation of Shandong (No. ZR2016FM28) and Double Hundred Plan Talent Project of Yantai.

REFERENCES

1. Yee, K. S., "Numerical solution of initial boundary value problems involving Maxwell's equations in isotropic media," *IEEE Trans. Antennas Propag.*, Vol. 14, No. 3, 302–307, 1966.
2. Chen, Y., R. Mittra, and P. Harms, "Finite-difference time-domain algorithm for solving Maxwell's equations in rotationally symmetric geometries," *IEEE Trans. Microw. Theory Tech.*, Vol. 44, No. 6, 832–839, 1996.
3. Ramadan, O., "Complex envelope Crank Nicolson PML algorithm for band-limited electromagnetic applications," *Electron. Lett.*, Vol. 42, No. 23, 2006.
4. Pursel, J. D. and P. M. Goggans, "A finite-difference time-domain method for solving electromagnetic problems with bandpass-limited sources," *IEEE Trans. Antennas Propag.*, Vol. 47, No. 1, 9–15, 1999.
5. Taflove, A. and S. C. Hagness, *Computational Electrodynamics: The Finite-Difference Time Domain Method*, 3rd Edition, Artech House, Norwood, MA, 2005.
6. Namiki, T., "3-D ADI-FDTD method unconditionally stable time-domain algorithm for solving full vector Maxwell's equations," *IEEE Trans. Microw. Theory Tech.*, Vol. 48, No. 10, 1743–1748, 2000.
7. Shibayama, J., M. Muraki, J. Yamauchi, and H. Nakano, "Efficient implicit FDTD algorithm based on locally one-dimensional scheme," *Electron. Lett.*, Vol. 41, No. 19, 1046–1047, 2005.
8. Fu, W. and E. L. Tan, "Development of split-step FDTD method with higher order spatial accuracy," *Electron. Lett.*, Vol. 40, No. 20, 1252–1254, 2004.
9. Ogurtsov, S. and G. Pan, "An updated review of general dispersion relation for conditionally and unconditionally stable FDTD algorithms," *IEEE Trans. Antennas Propag.*, Vol. 56, No. 8, 2572–2583, 2008.
10. Ju, S., K.-Y. Jung, and H. Kim, "Investigation on the characteristics of the envelope FDTD based on the alternating direction implicit scheme," *IEEE Microw. Wireless Compon. Lett.*, Vol. 13, No. 9, 414–416, 2003.
11. Sun, G. and C. W. Trueman, "Approximate Crank-Nicolson scheme for the 2-D finite-difference time-domain method for TEz waves," *IEEE Trans. Antennas Propag.*, Vol. 52, No. 11, 2963–2972, 2004.
12. Sun, G. and C. W. Trueman, "Unconditionally stable Crank-Nicolson scheme for solving two-dimensional Maxwell's equations," *Electron. Lett.*, Vol. 39, No. 7, 595–597, 2003.

13. Shi, X. Y. and X. Y. Jiang, "Implementation of the Crank-Nicolson Douglas-Gunn finite difference time domain with complex frequency-shifted perfectly matched layer for modeling unbounded isotropic dispersive media in two dimensions," *Microw. Opt. Technol. Lett.*, Vol. 62, No. 3, 1103–1111, 2020.
14. Sun, G. and C. W. Trueman, "Unconditionally-stable FDTD method based on Crank-Nicolson scheme for solving three-dimensional Maxwell equations," *Electron. Lett.*, Vol. 40, No. 10, 589–590, 2004.
15. Sun, G. and C. W. Trueman, "Efficient implementations of the Crank-Nicolson scheme for the finite-difference time-domain method," *IEEE Trans. Microw. Theory Tech.*, Vol. 54, No. 5, 2275–2284, 2006.
16. Tan, E. L., "Efficient algorithms for Crank-Nicolson-based finite-difference time-domain methods," *IEEE Trans. Microw. Theory Tech.*, Vol. 56, No. 2, 408–413, 2008.
17. Jiang, H. L., L. T. Wu, X. G. Zhang, et al., "Computationally efficient CN-PML for EM simulations," *IEEE Trans. Microw. Theory Tech.*, Vol. 67, No. 12, 4646–4655, 2019.
18. Wu, P., Y. Xie, H. Jiang, and T. Natsuki, "Performance enhanced Crank-Nicolson boundary conditions for EM problems," *IEEE Trans. Antennas Propag.*, Vol. 69, No. 3, 1513–1527, 2021.
19. Jiang, H. L., J. F. Zhang, W. X. Jiang, and T. J. Cui, "Unconditionally stable CN-PML algorithm for frequency-dispersive left-handed materials," *IEEE Ante. Wirel. Propag. Lett.*, Vol. 16, 2006–2009, 2017.
20. Xu, K., Z. Fan, D.-Z. Ding, and R.-S. Chen, "GPU accelerated unconditionally stable Crank-Nicolson FDTD method for the analysis of three-dimensional microwave circuits," *Progress In Electromagnetics Research*, Vol. 102, 381–395, 2010.
21. Rouf, H. K., "Improvement of computational performance of implicit finite difference time domain method," *Progress In Electromagnetics Research M*, Vol. 43, 1–8, 2015.
22. Long, S.-Y., W.-J. Chen, Q.-W. Liang, and M. Zhao, "A general ADE-FDTD with Crank-Nicolson scheme for the simulation of dispersive structures," *Progress In Electromagnetics Research Letters*, Vol. 86, 1–6, 2019.
23. Fajardo, J. E., J. Galván, F. Vericat, C. M. Carlevaro, and R. M. Irastorza, "Phaseless microwave imaging of dielectric cylinders: An artificial neural networks-based approach," *Progress In Electromagnetics Research*, Vol. 166, 95–105, 2019.
24. Wu, P. Y., Y. J. Xie, H. L. Jiang, et al., "Unconditionally stable higher order perfectly matched layer applied to terminate anisotropic magnetized plasma," *Inter. J. RF Micro. Comp.-Aided Engi.*, Vol. 33, No. 1, e22011, 2020.
25. Li, J. X. and P. Y. Wu, "Efficient PML implementation based on the unconditionally stable CN-FDTD algorithm for anisotropic magnetized plasma," *Optik*, Vol. 171, 468–475, 2018.
26. Chen, H. L. and B. Chen, "Anisotropic-medium PML for ADI-BOR-FDTD method," *IEEE Micro. Wirel. Compo. Lett.*, Vol. 18, No. 4, 221–223, 2008.
27. Li, J. X., W. Jiao, and X. M. Zhao, "Unconditionally stable CFS-PML based on CNAD-BOR-FDTD for truncating unmagnetized plasma," *IEEE Trans. Electro. Compat.*, Vol. 60, No. 6, 2069–2072, 2018.
28. Wu, P. Y., Y. J. Xie, H. L. Jiang, and L. Q. Niu, "Higher-order approximate CN-PML theory for magnetized ferrite simulations," *Advan. Theory Simulat.*, Vol. 3, No. 4, 2020.
29. Mukherjee, B. and D. K. Vishwakarma, "Application of finite difference time domain to calculate the transmission coefficient of an electromagnetic wave impinging perpendicularly on a dielectric interface with modified MUR-I ABC," *Defence Science Journal, DRDO*, Vol. 62, No. 4, 228–235, 2012.
30. Mukherjee, B., "Numerical solution in FDTD for absorbing boundary condition over dielectric surfaces," *Journal of Advance Research in Scientific Computing, IASR*, Vol. 4, No. 1, 13–23, 2012.
31. Berenger, J. P., "A perfectly matched layer for the absorption of electromagnetic waves," *J. Com. Phys.*, Vol. 114, No. 2, 185–200, 1994.

32. Berenger, J. P., *Perfectly Matched Layer (PML) for Computational Electromagnetics*, Morgan & Claypool, 2007.
33. Chew, W. C. and W. H. Weedon, "A 3D perfectly matched medium from modified Maxwells equations with stretched coordinates," *Microw. Opt. Technol. Lett.*, Vol. 7, No. 13, 599–604, 1994.
34. Kuzuoglu, M. and R. Mittra, "Frequency dependence of the constitutive parameters of causal perfectly matched anisotropic absorbers," *IEEE Microw. Guided Wave Lett.*, Vol. 6, 447–449, 1996.
35. Ramadan, O., "Unsplit field implicit PML algorithm for complex envelope dispersive LOD-FDTD simulations," *Electron. Lett.*, Vol. 43, No. 5, 2007.
36. Chen, J., J. G. Wang, and C. M. Tian, "Using weakly conditionally stable-body of revolution-finite-difference time-domain method to simulate dielectric film-coated circular waveguide," *IET Microw. Antennas Propag.*, Vol. 9, No. 9, 853–860, 2015.
37. Wu, P. Y., Y. J. Xie, H. L. Jiang, and L. Q. Niu, "Performance-enhanced complex envelope ADI-PML for bandpass EM simulation," *IEEE Micro. Wire. Compon. Lett.*, Vol. 30, No. 8, 729–732, 2020.
38. Nakazono, Y. and H. Asai, "Application of relaxation-based technique to ADI-FDTD method and its estimation," *2007 IEEE International Symposium on Circuits and Systems*, 1489–1492, 2007.
39. Farahat, N., J. Carrion, and L. Morales, "PML termination of conducting media in the finite difference time domain method for Bodies of Revolution (BORs)," *Workshop on Computational Electromagnetics in Time-Domain, 2005, CEM-TD 2005*, No. 96–99, Atlanta, GA, USA, 2015.
40. Appannagarri, N., et al., "Modeling phased array antennas in Ansoft HFSS," *Proceedings 2000 IEEE International Conference on Phased Array Systems and Technology (Cat. No. 00TH8510)*, 323–326, 2000.
41. Luo, K., S. Ge, L. Zhang, H. Liu, and J. Xing, "Simulation analysis of ansys HFSS and CST microwave studio for frequency selective surface," *2019 International Conference on Microwave and Millimeter Wave Technology (ICMMT)*, 1–3, 2019.
42. Tan, E. L., "Fundamental implicit FDTD schemes for computational electromagnetics and educational mobile apps (Invited review)," *Progress In Electromagnetics Research*, Vol. 168, 39–59, 2020.
43. Tay, W. C., D. Y. Heh, and E. L. Tan, "GPU-accelerated fundamental ADI-FDTD with complex frequency shifted convolutional perfectly matched layer," *Progress In Electromagnetics Research M*, Vol. 14, 177–192, 2010.
44. Tan, E. L., "Fundamental schemes for efficient unconditionally stable implicit finite-difference time-domain methods," *IEEE Trans. Antennas Propag.*, Vol. 56, No. 1, 170–177, 2008.
45. Singh, G., E. L. Tan, and Z. N. Chen, "Efficient complex envelope ADI-FDTD method for the analysis of anisotropic photonic crystals," *IEEE Photo. Techn. Lett.*, Vol. 23, No. 12, 801–803, 2011.
46. Singh, G., E. L. Tan, and Z. N. Chen, "Modeling magnetic photonic crystals with lossy ferrites using an efficient complex envelope alternating-direction-implicit finite-difference time-domain method," *Opt. Lett.*, Vol. 36, 1494–1496, 2011.
47. Heh, D. Y. and E. L. Tan, "Unconditionally stable multiple one-dimensional ADI-FDTD method for coupled transmission lines," *IEEE Trans. Antennas Propag.*, Vol. 66, No. 12, 7488–7492, 2018.
48. Yang, Z. and E. L. Tan, "Efficient 3-D fundamental LOD-FDTD method incorporated with memristor," *IEICE Trans. Electronics*, Vol. E99-C, No. 7, 788–792, 2016.
49. Heh, D. Y. and E. L. Tan, "Some recent developments in fundamental implicit FDTD schemes," *Asia-Pacific Symp. Electromag. Compat.*, 153–156, Singapore, 2012.
50. Yang, Z., E. L. Tan, and D. Y. Heh, "Variants of second-order temporal-accurate 3-D FLODFDTD schemes with three split matrices," *IEEE Int. Conf. Comput. Electromagn.*, 265–267, Guangzhou, 2016.